Supplementary content

Table S1 Selected experimental and calculated[a] IR frequencies (in cm^{-1}) and IR intensities (I, in km mol^{-1}) of $[NiL_2]^{2+}$

Num.	Exp.	Calc. Freq. (I)[b]	Assignment
153	3472	3570(130)	NH_2 unsym str.
150	3367	3436(290)	NH_2 sym str.
148	3291	3391(7)	NH str.
141	3120	3127 (13)	unsym C-H str. py
139	3053	3047(23)	unsym CH_2 str. amide
134		3039(26)	unsym CH_2 str. amide
133	2957	2982(8)	sym CH_2 str. amide
130	2933	2976(51)	sym CH_2 str. picolyl
128	2886	2884(30)	sym CH_2 str. amide
126	1657	1639(807)	C=O str. amide
125		1593(88)	C=C str. py
122	1609	1568(540)	NH_2 bend.
121	1547	1561(54)	C=C str. py
118	1489	1483(16)	CH_2 bend. amide
116		1471 (13)	CH_2 bend Picolyl
115		1462 (45)	CH_2 bend Picolyl
112	1453	1453(131)	OC-CH_2 bend.
110	1434	1438 (19)	CH_2 Picolyl – NH twis .
108		1427 (18)	C-H py. twis
107		1420 (128)	HN-CH_2 bend+CH_2 bend.+CH twis
102	1374	1369(18)	CH_2 rock. Picolyl
101	1324	1332 (37)	CH_2 rock. amide
99	1322	1302 (31)	CH_2 twis Picolyl + C-H rock Py
96	1290	1277 (16)	H-CCH- scis. amide
95	1261	1271(27)	H-CC-H- scis. amide
92	1249	1244(15)	CH_2 twis. amide and Picolyl
82	1046	1091(30)	NH_2 and CH_2 rock.
81		1084(8)	NH_2 rock.
69	965	997(86)	H-CCH rock. py
65		956(44)	CH_2 twis. amide and Picolyl
63	846	942(155)	N-H and CH_2 bend. picolyl
59	819	817(70)	CH_2 twist. amide
	771	786(50)	NH_2 and CH_2 rock.
	734	747(308)	NH_2 wagg.
	690	681(154)	NH_2 wagg.

Table S2 Selected experimental and calculated[a] IR frequencies (in cm^{-1}) and IR intensities (I, in km mol^{-1}) of $[ZnL_2]^{2+}$

Num.	Exp.	Calc. Freq. (I)[b]	Assignment
153	3471	3573(85)	NH_2 unsym str.
152	3446	3572(45)	NH_2 unsym str.
150	3358	3437(276)	NH_2 sym str.
149	3291	3343(3)	NH str.
142	3296	3221(11)	unsym C-H str. py
140	3257	3190(12)	unsym C-H str. py
139	3033	3016(11)	unsym CH_2 str. amide
134		3005(26)	unsym CH_2 str. amide
131	2953	2941(30)	sym CH_2 str. picolyl
130	2922	2939(12)	sym CH_2 str. amide
129	2890	2937(30)	sym CH_2 str. amide
128	2893	2894(11)	sym CH_2 str. picolyl
126	1661	1623(807)	C=O str. amide
125	1583	1575(50)	C=C str. py
123	1609	1556(526)	NH_2 sciss.
122		1543(9)	C=C str. py
119	1486	1466(13)	CH_2 sciss. amide
117	1448	1445 (20)	CH_2 bend Picolyl
115	1414	1439 (72)	OC-CH_2 bend.
114	1453	1453(28)	CH_2 bend picolyl
113		1425(10)	CH_2 rock + NH bend .
111		1417 (17)	CH_2 bend picolyl
109		1408 (18)	C-H py. twis
107	1373	1373 (12)	CH_2 rock. Picolyl
105		1362(11)	HN-CH_2 bend
104		1357 (11)	CH_2 twist. amide+CH_2 trock.picolyl
103		1346 (38)	CH_2 rock Picolyl + C-H rock Py
101	1320	1321 (32)	amide
100	1296	1314(33)	CH_2 twis. + CH_2 rock. amide
98	1284	1286(16)	CH bend. Py
96	1258	1258(15)	CH_2 rock. amide and CH_2 rock. picolyl
94	1204	1243(15)	CH_2 twist. amide and CH_2 twist. picolyl
84		1079(16)	NH_2 and CH_2 rock.
80		1052(37)	H-CCH rock. py
74	960	983(30)	CH_2 rock. amide and HN-CH_2 str.
69		948(104)	N-H and CH_2 bend. picolyl
65		923(51)	CH_2 twist. amide
62	847	847(203)	NH and CH_2 rock.
57	785	793(308)	C-C bend. py.
52	765	768(62)	NH_2 rock +CH_2 rock.
51	734	740(308)	C-H wagg. Py
47	684	674	NH_2 wagg.

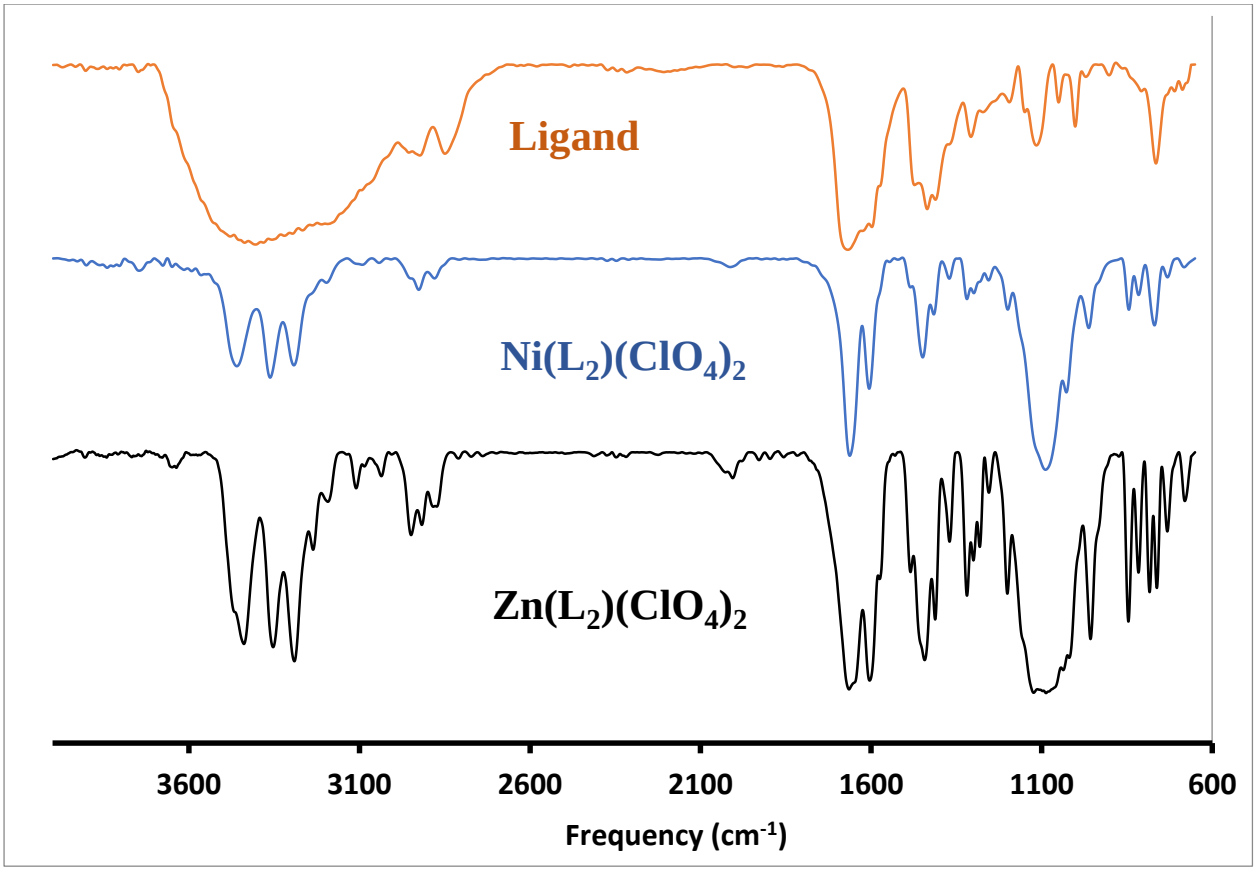

Fig. S1 IR spectra of the ligand, $[ZnL_2](ClO_4)_2$, and $[NiL_2](ClO_4)_2$

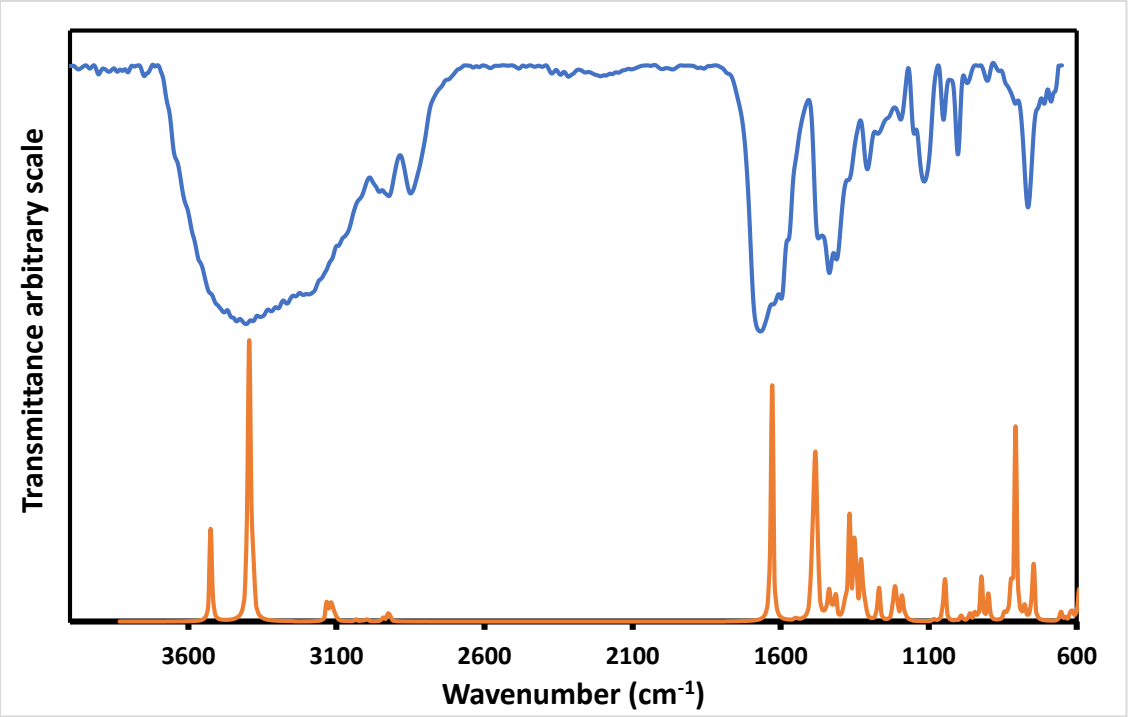

Fig. S2 FT-IR spectra of ligand (top), and calculated IR for ligand at B3LYP/LanLD2Z level of theory (bottom)

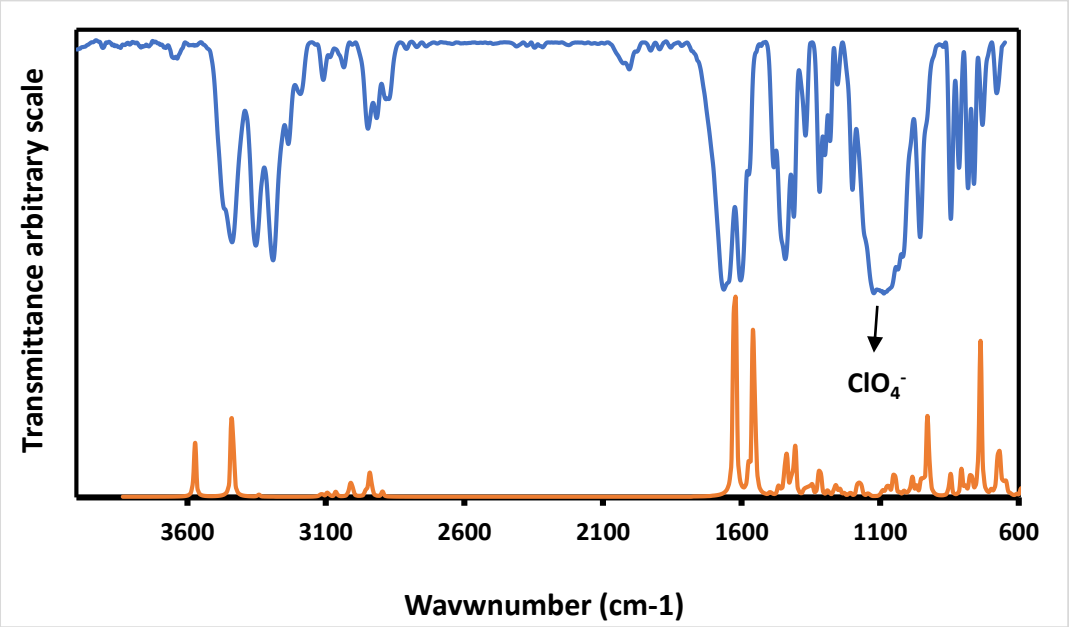

Fig. S3 FT-IR spectra of ligand and complexes (top), as well as calculated IR for $[ZnL_2](ClO_4)_2$ at B3LYP/LanLD2Z level of theory (middle) and IR-graphical correlation between experimental and DFT analysis (bottom)

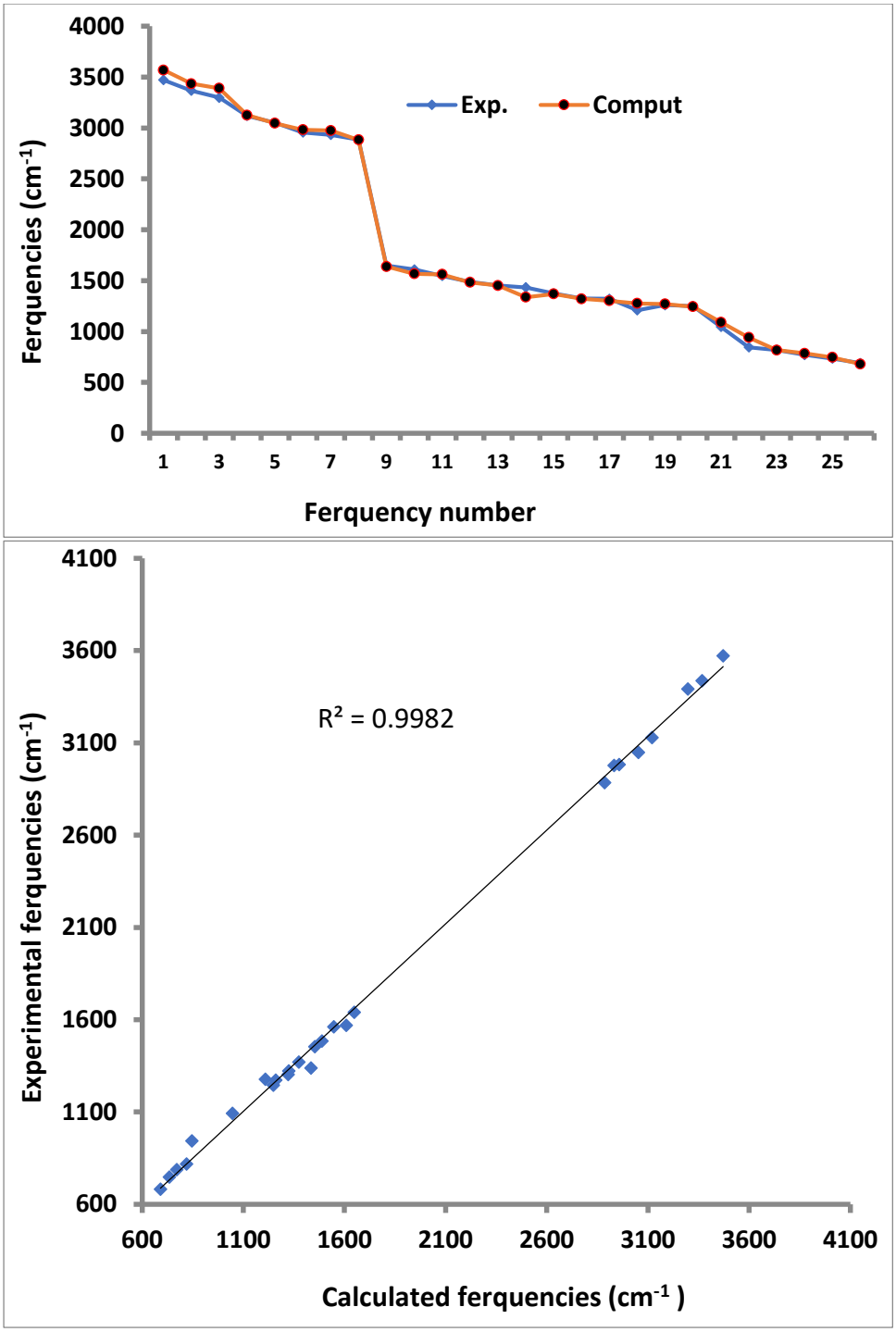

Fig. S4 Analysis graph of the calculated vibrational frequencies versus the experimental ones for $[NiL_2]^{2+}$

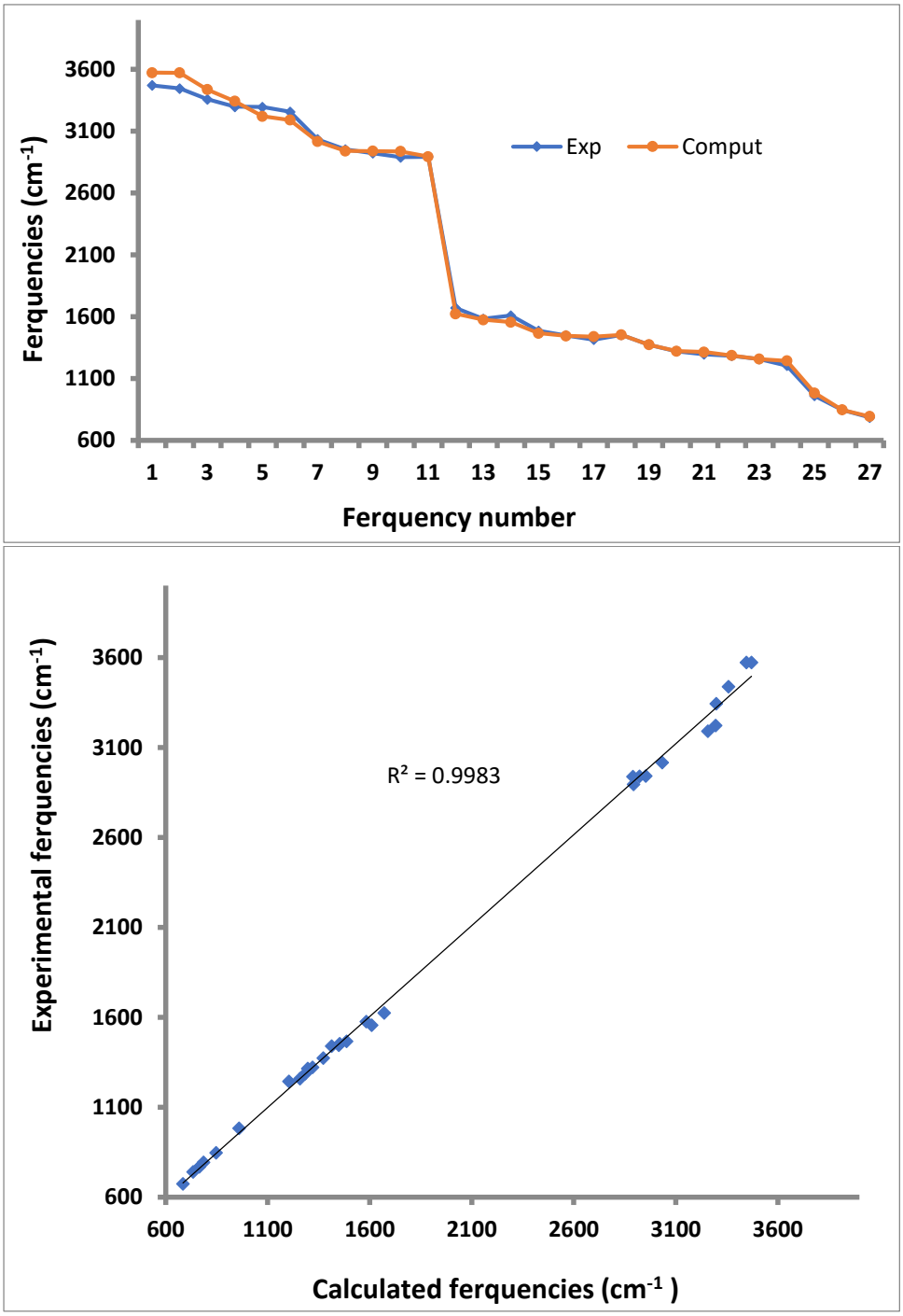

Fig. S5 Analysis graph of the calculated vibrational frequencies versus the experimental ones for $[ZnL_2]^{2+}$

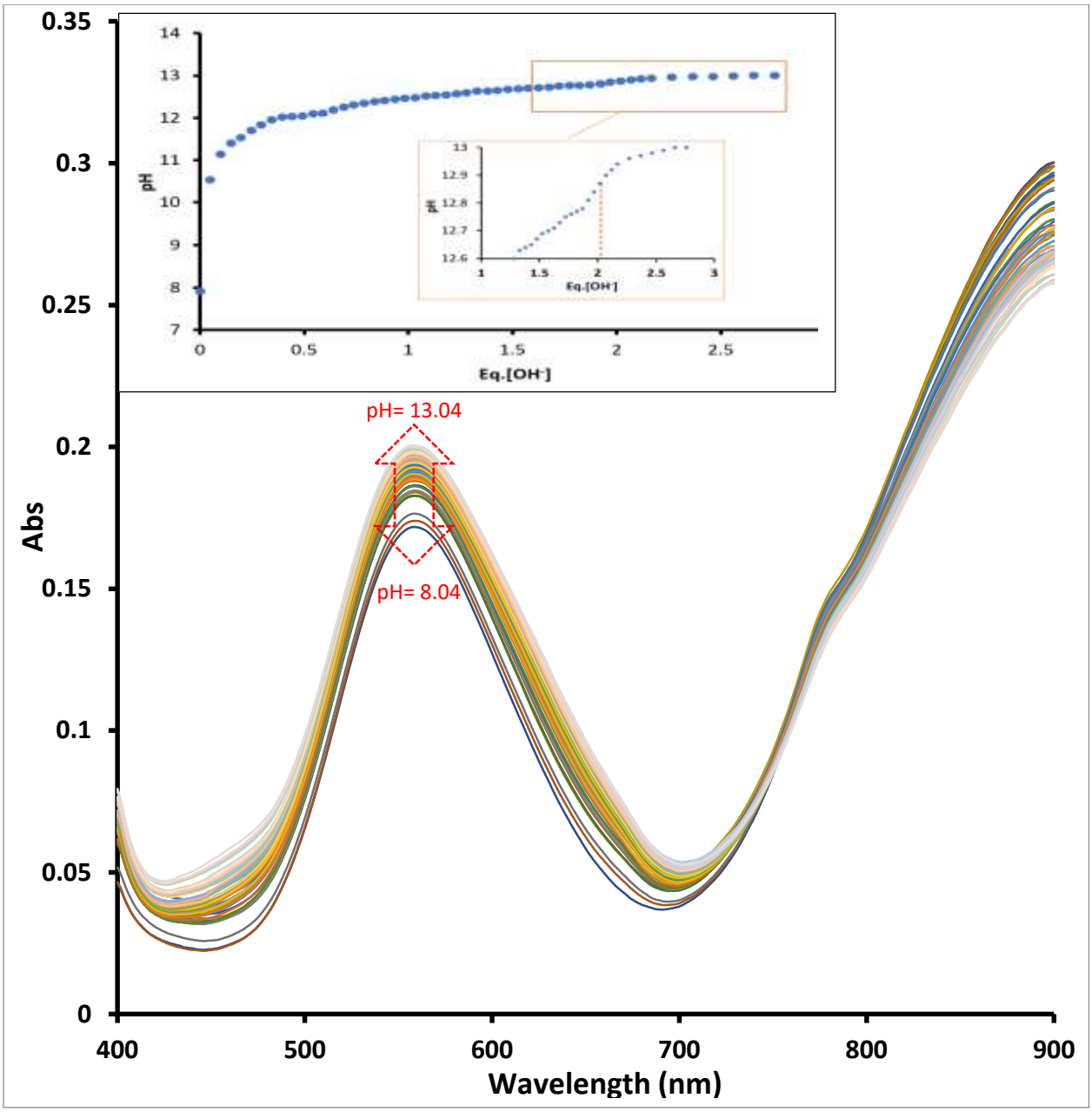

Fig. S7 The pH-dependent visible spectra of [NiL_2] in aqueous solution at 25 °C. The inset graph shows the pH versus equivalent [OH^-] at 560 nm on titration (4 mM in H_2O) with NaOH (0.01M). (pH= 8.04–13.00)

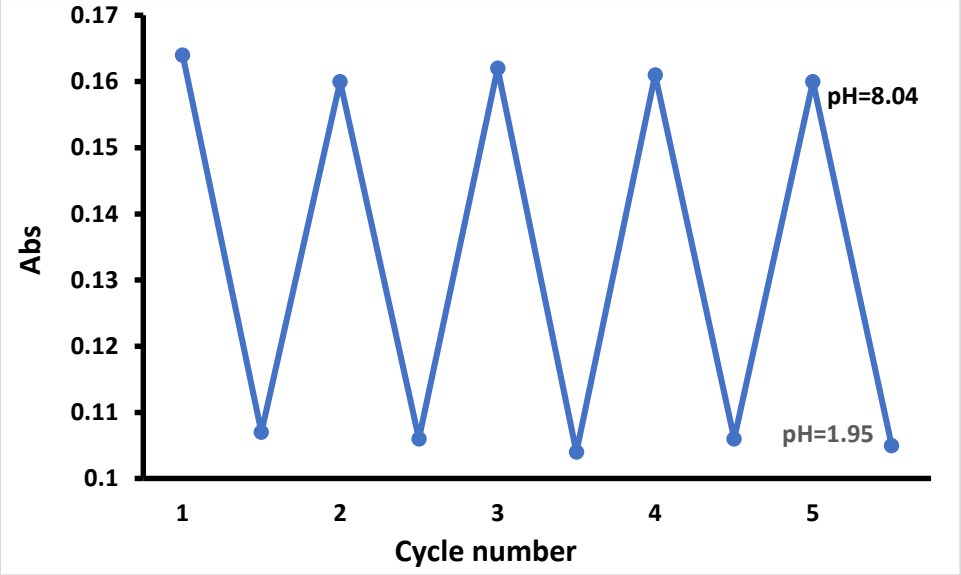

Fig. S8. The absorbance changes of complex **1** over a pH range of 8.04-1.95 after five cycles. The absorbance values were corrected due to the addition of acid and the change in the concentration of the solution.

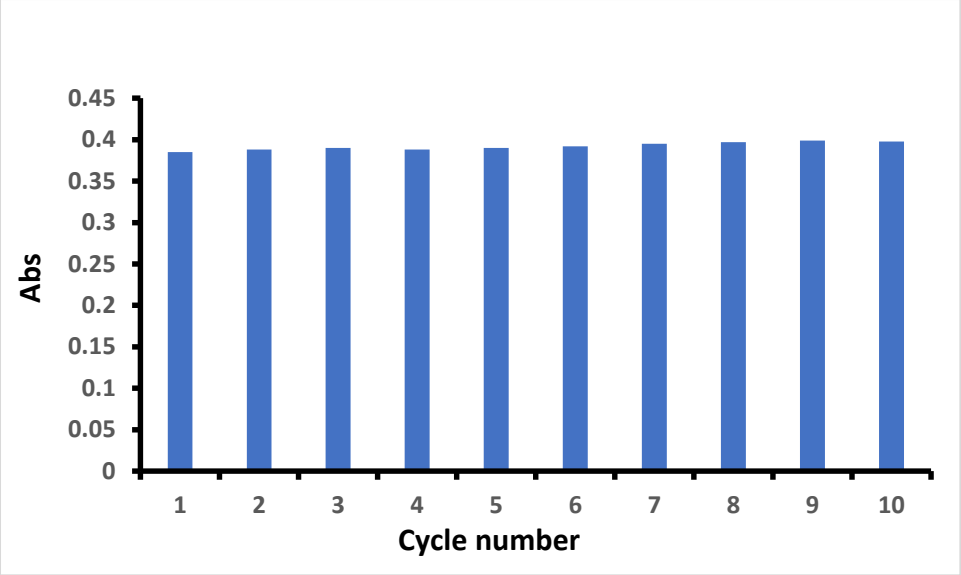

Fig. S9. The absorbance changes (at 661 nm) of complex 1 after being heated and cooled in DMSO for 10 cycles. The volume of the solution was kept constant by the addition of solvent.

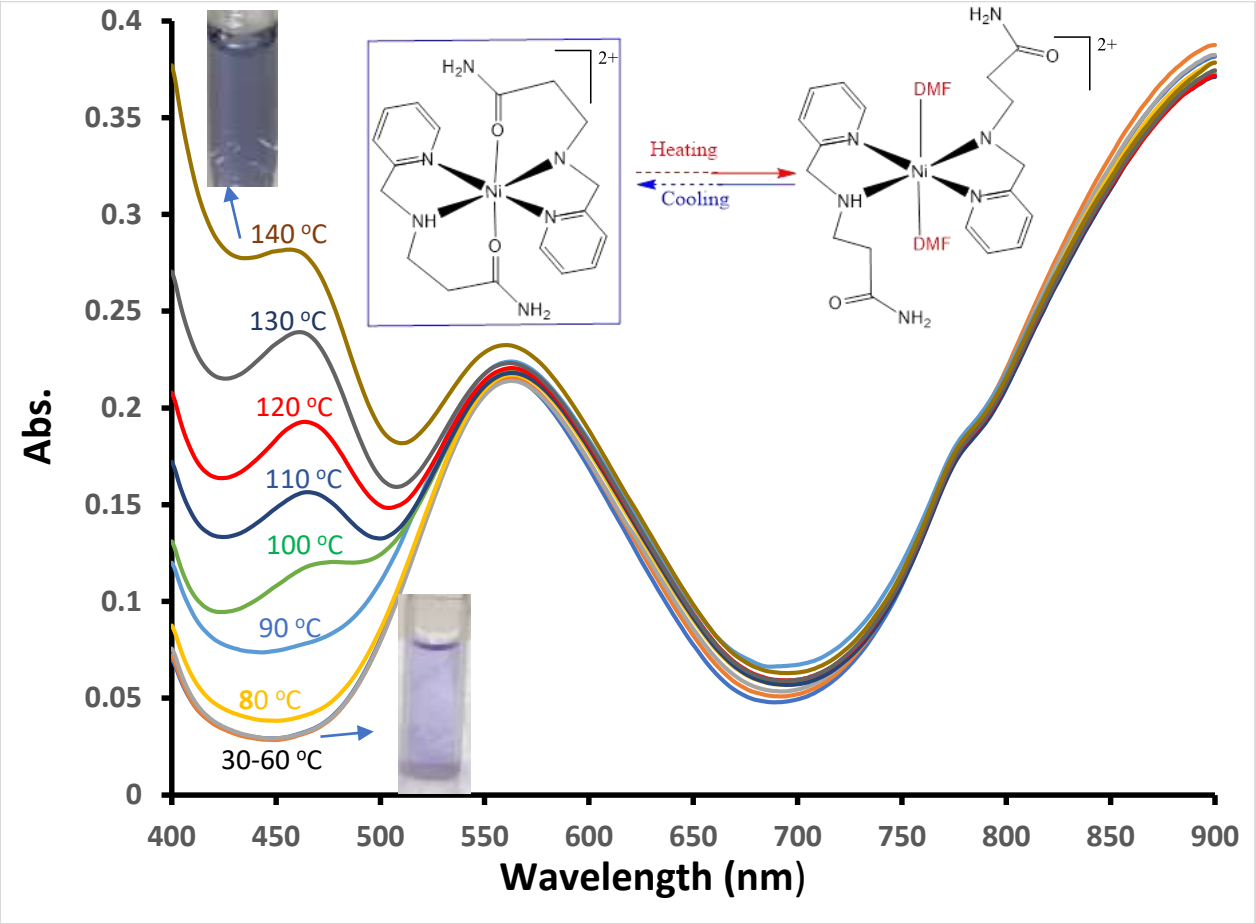

Fig. S10 Temperature dependence of the visible absorbance of DMF solution of $[NiL_2]^{2+}$. Inset figure structural change of the complex in solvents of DMF upon heating and cooling